

# Chemical and Mechanical Evaluation of Bio-composites Based on Thermoplastic Starch and Wood Particles Prepared by Thermal Compression

María Guadalupe Lomelí-Ramírez,<sup>a,\*</sup> Arturo Javier Barrios-Guzmán,<sup>b</sup> Salvador García-Enriquez,<sup>c</sup> José de Jesús Rivera-Prado,<sup>a</sup> and Ricardo Manríquez-González<sup>a</sup>

The present work inspects the preparation of bio-composites of cassava starch with particles of eucalyptus wood through the application of a novel method of thermal compression. Bio-composites with different amounts of wood particles (5 to 30%), with particle sizes of 4 and 8 mm, were obtained. Chemical and mechanical evaluation of these samples was carried out using optical microscopy, infrared spectroscopy (FTIR), X-ray diffraction (XRD), scanning electron microscopy (SEM), and the moisture absorption effect. The effect of the amount and size of the wood particles was tested by comparison with a thermoplastic matrix sample. Results from these evaluations demonstrated that the thermo-compression method produced bio-composites with a distribution of particles in the matrix that contributed to an increase in their tensile strength. This mechanical property is also enhanced by interfacial adhesion between the matrix and particles, as confirmed by SEM. Furthermore, the maximum amount of particles in the bio-composites (30%) showed the maximum resistance to moisture absorption. Temperature and time parameters contributed to the formation of diffraction patterns  $V_H$  and  $E_H$  as a consequence of the structural disruption of native starch. Finally, FTIR showed the chemical compatibility between the starch, glycerol, and wood particles.

*Keywords:* Bio-composites; Thermoplastic starch; Wood particles; Thermal compression

*Contact information:* a: Departamento de Madera, Celulosa y Papel, Centro Universitario de Ciencias Exactas e Ingenierías, Universidad de Guadalajara, Km 15.5, Carretera Guadalajara-Nogales, Zapopan, Jalisco, México, CP. 45220; b: Departamento de Ingeniería Química, Centro Universitario de Ciencias Exactas e Ingenierías, Bld. Marcelino García Barragán 1451, Guadalajara, Jalisco, México CP. 44430; c: Ingeniería-Básicas, Centro de Enseñanza Técnica Industrial, Nueva Escocia 1885, Guadalajara, Jalisco, México CP.44638; \*Corresponding author: glomeli@dmcyp.cucei.udg.mx

## INTRODUCTION

Starch is a natural polymer obtained from plants and composed chemically of amylose (20 to 30%) and amylopectin (70 to 80%) carbohydrates. These structures are formed by glucopyranose units connected with  $\alpha(1-4)$  glycosidic bonds in a spiral chain and in linear and branched forms, respectively. Because starch is a natural polysaccharide with multiple botanical sources, it is considered to be a biodegradable, renewable, sustainable, and low-cost material. All of these benefits promote the potential use of this polysaccharide in papermaking additives, textiles, adhesives, thermoplastic starch (TPS) (Avérous and Halley 2009) for producing packing containers, eating utensils, and as raw material for film preparation (Vilaseca *et al.* 2007). The thermoplastic property is obtained when native starch is processed in the presence of a plasticizer at high

temperatures and mechanical shear (Mo *et al.* 2011). This thermoplastic process is achieved when semi-crystalline starch becomes amorphous because of the substitution of the original hydrogen bonds between the amylose and amylopectine by the plasticizer (Prachayawarakorn *et al.* 2010). A plasticizer (*e.g.*, glycerol, triethylene glycol, or oleic acid) with a high boiling point, in combination with starch, can be processed in a manner similar to a conventional synthetic thermoplastic (Corradini *et al.* 2006). However, this TPS has a lower mechanical strength in comparison with synthetic versions. Thus, to increase this mechanical property, natural fibers are added to reinforce the material. Some studies concerned with this issue have used cotton fibers (Prachayawarakorn *et al.* 2010), cellulose crystals from bamboo (Liu *et al.* 2008), and cellulose fibers from wood (Duanmu *et al.* 2010). The addition of natural fibers as a way to reinforce biodegradable polymers promotes the potential functionality and technological application due to their low cost, high availability, biodegradation, and considerably high resistance (Espinach *et al.* 2014). The amount of fibers used in the total weight of the thermoplastic is between 5 and 30%.

Because starch in the matrix (mixture with plasticizer) and fibers are obtained from natural sources, the resulting material is considered a bio-composite or “green” composite because it is completely biodegradable. Bio-composites are light materials and show good rigidity; however, the mechanical properties of the reinforced materials, such as the impact resistance, can be negatively affected when they absorb a certain amount of moisture (Kuciel and Liber-Knec 2009). Some approaches to overcome these problems have used chemical modification of the materials, mixtures of natural and non-biodegradable conventional polymers, as well as reinforcing the thermoplastics with inorganic materials and natural fibers (Corradini *et al.* 2006). The properties of composites reinforced with fibers depend on several factors, such as adhesion of the matrix and the amount and orientation of the fibers. Corradini *et al.* (2006) improved the matrix-fiber adhesion by chemically and mechanically modifying natural fibers used in composites.

Currently, the field of polymeric matrices reinforced with natural fibers is in constant development and is focused on composites prepared with biodegradable polymers and fibers, which furthers the objective of producing materials that are environmentally friendly (Vilaseca *et al.* 2007). Moreover, there is a growing interest in using these materials to replace plastic materials reinforced with synthetic fibers in a wide range of industrial applications, such as automotive, packing, and furniture production. In general, fibers based on cellulose, such as cotton, flax, hemp, henequen, jute, and timber, are commonly used for reinforcing plastics because of their high resistance, rigidity, and low density (Alemdar and Sain 2008). In light of this, preparation of TPS has been carried out by injection, extrusion, electrospinning, blow moulding, Haake torque rheometer, and polymer solution casting (Corradini *et al.* 2006). Another novel way to prepare TPS materials with direct thermoplastification by compression was recently developed and patented by Lomelí-Ramírez *et al.* (2011). In comparison with the traditional processes for moulding plastics described above, this new method offers several advantages: (1) the required equipment is cheaper, (2) the process of plasticization is achieved in one step, (3) the high viscosity of the thermoplastic starch is not a problem, and (4) the fibers are homogeneously incorporated with the matrix as well as textiles (*e.g.*, jute).

In the present work, this new methodology for preparing thermoplastic cassava starch, reinforced with different sizes and amounts of eucalyptus particles, is applied. The

chemical and mechanical properties of the bio-composites were evaluated using optical microscopy, infrared spectroscopy (FTIR), X-ray diffraction (XRD), scanning electron microscopy (SEM), and the moisture absorption effect. From the results of this study, important information concerning the practical application and use of this methodology in similar bio-composites and new, biodegradable materials with desirable physicomechanical properties can be identified. Therefore, this process could be promising for diverse industrial purposes and from an environmental point of view.

## EXPERIMENTAL

### Material

The native cassava starch (*Manihot esculenta*) used in this study was donated by the J. A. Pasquini Company. Eucalyptus wood (*Eucalyptus grandis*) was used to produce the biocomposites. The commercial grade glycerol used as a plasticizer was donated by the Labsynth Company.

### Preparation of Composites

Eucalyptus wood samples were milled and sieved to obtain particle sizes of  $4 \pm 1$  and  $8 \pm 1$  mm of length with width averages of 0.5 mm and 1 mm, respectively. Separately, cassava starch was mixed thoroughly with 30 wt.% glycerol in a plastic bag until attaining a homogeneous powdered mixture, which was used to prepare the biocomposites. Then, the wood particles (5, 10, 20, and 30 wt.%) were blended with this mixture by a 5 L mixer (Hobart model N50, São Paulo, Brazil). The prepared mixtures were poured into a stainless steel mold with a size of 170 mm  $\times$  170 mm  $\times$  3 mm, which was placed into a hydraulic press with an applied pressure of 40.25 MPa for about 50 min at 160 °C; a controlled cooling apparatus was also used to obtain the laminate TPS composites. A laminate matrix sample was also prepared as a reference.

### Optical Microscopy

A Zeiss stereoscopic microscope (Discovery VI2, Jena, Germany) equipped with a Zeiss AxioCam camera was used to observe the transparency obtained in the composites and the distribution of eucalyptus wood particles in the composites.

### Mechanical Testing

Tensile samples of the matrix and the composites were cut from respective laminates (plaques) using a laser cutting machine Gravograph LS100 (São Paulo, Brazil). The samples obtained were tested in a universal testing machine (EMIC DL 20.000 Paraná, Brazil) following the standard ASTM D 638M-96 (1998) procedure, at room temperature and a testing speed of 5 mm/min. Six to seven specimens were tested for each sample, and the average values of the tensile properties were recorded. All of the specimens were dried for 5 h at 60 °C in a laboratory oven and then kept in a desiccator prior to being tested.

### Scanning Electron Microscopy (SEM)

A Philips XL-30 (North Billerica, MA) scanning electron microscope with an operating voltage of 10 to 20 kV was used to obtain SEM micrographs taken from fractured tensile test samples of both the matrix and composites. For this purpose, all

samples (without special treatment) were coated with gold by sputtering in a vacuum chamber before observation.

### X-ray Diffraction (XRD)

X-ray diffraction (XRD) studies were carried out using a Shimadzu diffractometer (Model XRD 7000; Kyoto Japan), with monochromatic Cu K $\alpha$  radiation ( $k = 1.5418\text{\AA}$ ), at operation conditions of 40 keV and 20 mA, to determine the crystallinity of the materials. Samples were dried at 60 °C for 8 h, and the dimensions of the composite specimens used were 40 x 20 x 3 mm; the starch sample was measured in powdered form. The analysis was carried out in the  $2\theta$  angle range of 2.5° to 60° with a scanning speed of 1°/min.

### Moisture Absorption

To assess the sensitivity of the bio-composites to moisture, humidity sorption isotherms of the composites were obtained. For this purpose, the samples were first dried in an air circulating oven at 60 °C. The samples were then conditioned at 0.004 wt% by keeping them in a desiccator at 22 to 25 °C and a relative humidity of  $75 \pm 2\%$  using a saturated solution of sodium chloride (NaCl) that was prepared according to the ASTM E 104-2 (2007) standard. The samples were taken out daily to check the water absorption as a function of time until the weight became constant. The moisture content was calculated using the equation,

$$\text{Moisture content (\%)} = [(M_1 - M_0) / M_0] 100, \quad (1)$$

where  $M_0$  and  $M_1$  correspond to the mass of the samples (in g) before and after the oven thermal treatment at certain periods of time, respectively.

### FTIR Analysis

FTIR spectrum analysis of the native starch was carried out using Bio-Rad FTIR equipment (Excalibur model FTS 3500GX; Cambridge, MA) with the potassium bromide disk technique. The FTIR analyses of the bio-composite samples were performed in a Bruker Vertex-70 (Bruker Optics, Germany) spectrophotometer using the attenuated total reflectance (ATR) technique. All IR spectra were then averaged out of 64 scans with a resolution of  $4\text{ cm}^{-1}$  within a frequency range of 4000 to  $700\text{ cm}^{-1}$ .

## RESULTS AND DISCUSSION

### Optical Microscopy

In Fig. 1, the micrographs of bio-composites prepared with particle sizes of  $8 \pm 1$  mm (a, b, and c) and  $4 \pm 1$  mm (d, e, and f) are shown. The biocomposite samples observed in Fig. 1b and 1e correspond to thermoplastic material with a eucalyptus amount of 5%, and the samples shown in c and f were prepared with 20% eucalyptus particles. To analyze the thermoplastics in greater detail, enlargements of samples in Figs. 1b and 1e were made (Figs. 1a and 1d, respectively). As can be observed in all samples, an even distribution of wood particles in the thermoplastic starch matrix is clearly evident due to the obtained transparency. According to Canevarolo (2006),

transparency of the thermoplastic is attained when the semi-crystalline starch is disrupted by plasticizer, temperature, mechanical shear, and pressure. Moreover, Fig. 1 shows the compatibility of the reinforcing material with the matrix and the organization of the wood particles in the bio-composites. Guimarães *et al.* (2010) prepared composites of corn starch and banana fibers *via* thermo moulding. In the Guimarães *et al.* (2010) study, the authors reported the formation of air bubbles during the moulding process that may have formed by the evaporation of water. In the present study, the absence of bubbles in the samples, which can produce defects in the composite, confirmed the success of the preparation and viability of the process. In addition, the methodology applied to prepare bio-composites in the present work avoids problems such as fluidity by high viscosity in the processing of the thermoplastic starches by extrusion and injection (Ma *et al.* 2005).



**Fig. 1.** Micrographs of bio-composites with eucalyptus particle sizes of 8 mm (a-c) and 4 mm (d-f) and amounts of 5% (b, e) and 20% (c, f). Micrographs (a) and (d) correspond to enlargements of samples (b) and (e), respectively.

### Mechanical Testing

The results of mechanical testing of the tensile resistance of the bio-composites are shown in Table 1. Data regarding differences in strength and elongation were obtained with respect to the amount and sizes of particles. The tensile strength improved when the amount of wood particles increased, as can be observed in samples that contained 30% wood particles, as well as when the size of the particles was smaller. In contrast, the strain decreased with increasing amount and size of thermoplastic starch. This may be due to strong adhesion at the interface between the matrix and the smaller sized particles. Wicaksono *et al.* (2013) reported on the strengthening mechanisms associated with the ability of the fiber to form a network structure of the film matrix and attributed it to the high surface area contact of the smaller fibers. These results for the bio-composites are also corroborated with SEM micrographs (Fig. 2f). In addition, the

high surface area of fibers promotes the formation of hydrogen bonds between matrix films and particles. Bilbao-Sainz (2011) found that enhancement of hydrogen bond formation can lead to higher efficiency in the stress transfer from the matrix to the fibers.

**Table 1.** Results of Tensile Properties of Matrix and Bio-composites

Materials	Tensile strength (MPa)		Elastic modulus (MPa)		Elongation (%)	
	8 ± 1 mm	4 ± 1 mm	8 ± 1 mm	4 ± 1 mm	8 ± 1 mm	4 ± 1 mm
Matrix	1.9 (0.3)a		110.7 (3.4)a		53.5 (3.4)a	
5% wood	2.4 (0.2)ab	2.8 (0.2)cd	148.5 (9.1)a	221.4 (8.3)b	36.0 (4.0)b	25.7 (5.4)c
10% wood	2.8 (0.2)bc	3.7 (0.2)de	249.0 (7.9)bc	366.2 (9.8)d	23.0 (4.9)cd	19.9 (2.5)d
20% wood	3.9 (0.4)ef	4.4 (0.5)f	391.5 (8.2)d	607.9 (7.6)e	18.6 (2.7)d	11.7 (2.4)e
30% wood	4.5 (0.7)f	6.0 (1.1)g	654.0 (8.1)e	778.8 (7.8)f	13.3 (2.5)e	10.2 (1.9)e

Numbers in parenthesis are standard deviations

Different letters, Significant at the 95.0% confidence level

It is well known that the geometry of a fiber, *i.e.*, its morphology, architecture, orientation, arrangement, and volume fractions, influences the mechanical properties of composites. Of these factors, the volume fraction is one of the most important because many mechanical properties increase because of higher reinforcement loading; however a sufficiently high amount of the reinforcing material can also cause agglomeration and low dispersion of the fibers in the matrix (Fowler *et al.* 2006).

Ma *et al.* (2005) attributed the increase in strength properties to the fact that the matrix of TPS melts involving the fibers. Another factor was the intrinsic fiber-matrix adhesion caused by the chemical similarity between starch and the cellulose fiber. Also, the differences in performance of the composites suggest that the conditioning treatment used (60 °C for 5 h) in the present study was able to affect the function of the plasticizer, causing the starch chains to have better packing, resulting in better organization due to more intense interactions of macromolecules (amylase and amylopectin), which has been reported in previous studies (Lomelí *et al.* 2011). Chakraborty *et al.* (2007) showed the same effect by placing samples at 80 °C for 24 h and mentioned that the materials under these conditions showed better mechanical properties in relation to the composites conditioned at a relative humidity of 50%.

Guimarães *et al.* (2010) reported values from 1.7 to 4.3 (MPa) for tensile strength, 24.6 to 484.0 (MPa) for elasticity modulus (MOE), and 1.20 to 75.56% elongation for corn starch bio-composites reinforced with various proportions of banana fiber and sugar cane bagasse fibers. Müller *et al.* (2009) reported values between 1.59 and 26.6 (MPa) for tensile strength, 11 and 1047 (MPa) for modulus of elasticity, and 13 to 101% elongation for cassava starch films with various proportions of eucalyptus pulp fibers prepared by the casting method. The different values reported in the literature depend on the type of starch (native or modified), the processing method (*e.g.*, injection, molding, extrusion, casting), the amount, and the kind of reinforcement (*e.g.*, fiber, pulp, wood). Thus, the correct choice of the components in the bio-composites can contribute to improving mechanical properties such as tensile strength and modulus of elasticity.

### Scanning Electron Microscopy (SEM)

Figure 2 shows a series of SEM micrographs of the fractured surface of tensile tested specimens of composites containing different amounts of wood particles. Bio-



composites with a eucalyptus particle size of 8 mm and with contents of 5 and 30% are depicted in Figs. 2a and 2b, respectively. In Fig. 2b, empty spaces produced from the mechanical detachment of the wood particles after the tensile stress essay can be observed, which implies a weak adherence between the particles and the matrix. Figure 2c shows, in detail, interfacial zones between the wood particles and matrix (indicated by arrows) of the 30% sample, where a small contact area between them can be seen. It is well known that the interface between the matrix and reinforcing material in composites is responsible for transferring the tensile stress from the matrix to the reinforcing material during mechanical strain. In other words, the tensile strength of these materials is attributed to the adherence between the components of the composites, as well as the intrinsic properties of the reinforcing material and polymer used (Kuciel and Liber-Knec 2009).

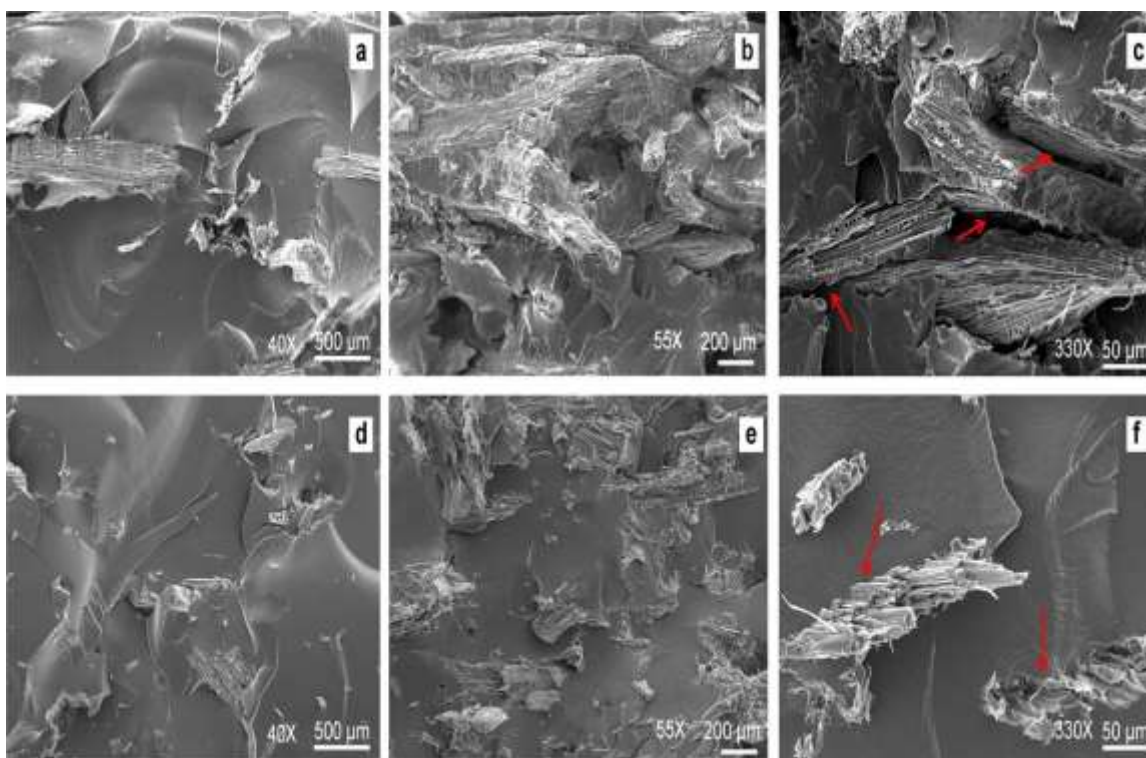


**Fig. 2.** SEM micrographs of fractured surface of bio-composites: (a) 5%, (b) 30%, and (c) detail of wood-matrix interface, particle size of 8 mm; (d) 5%, (e) 30%, and (f) detail of wood-matrix interface, particle size of 4 mm.

Figures 2d and e correspond to bio-composites prepared with a eucalyptus particle size of 4 mm and with a content of 5 and 30% as well. A smooth and homogeneous surface with evenly distributed wood particles in the matrix may be observed in these micrographs. Because of the small size of the particles (4 mm) in those bio-composites, it is possible to achieve a greater contact area (continuous phase) with the TPS. In this case, there were fewer empty spaces present after the tensile stress testing than there were with the bio-composite with a particle size of 8 mm. In Fig. 2c, it can be seen that the wood particles adhered well to the matrix, in accordance with the tensile strength data obtained for these samples (Table 1). This result suggests that the bio-composites with small particle sizes (4 mm) yielded better mechanical properties because they had a higher

contact area than the 8-mm particles. According to Fowler *et al.* (2006), a reinforcing effect will be achieved when adherence between the reinforcing material and polymer matrix is good.

### X-ray Diffraction (XRD)

In Fig. 3a, the XRD patterns of wood, native starch, and composites with a particle size of 8 mm are shown. Figure 3b corresponds to composites prepared with a particle size of 4 mm and a matrix sample. The native starch is partially crystalline (15 to 45%), and two polymorphic forms, A and B, were present. In addition, C, an intermediate polymorphic form, was also present (Ma *et al.* 2005). Cassava starch showed diffraction at angles of ( $2\theta$ ) 15.2°, 20.1°, 23.1°, and a doublet at 17.2° and 18.1°, which have been reported by Kawabata *et al.* (1984). These measurements corresponded to crystallinity type  $C_A$  due to a 90% type A crystallinity and 10% type B crystallinity (Zobel 1988). Granular destruction, caused by the direct plasticization process in the press through the application of temperature, pressure, and a plasticizer, resulting in changes to the characteristic profile of the native starch (type- $C_A$ ) in relation to type- $E_H$  and type- $V_H$ , as reported by Van Soest *et al.* (1996), can be observed in Fig. 3a and b. According to these authors, processing temperature, residence time, and cooling speed affect the final crystallographic pattern of starch-based materials. Accordingly, type- $E_H$  crystallinity is promoted when residence time and temperature are increased. Therefore, in this study, the time and temperature used during processing may have contributed to the formation of  $V_H$  and  $E_H$  diffraction patterns, as was previously reported by Lomelí-Ramírez *et al.* (2014). Also, Teixeira *et al.* (2009) reported that bio-composite samples display a diffraction peak around  $2\theta=16.8^\circ$ , characteristic of amylopectin recrystallization, *i.e.*, B-type crystallization. The diffraction peak corresponding to cellulose wood at  $2\theta=22.5^\circ$  was clearly observed in the diffraction patterns of the bio-composites. As the amount of wood particles increased in the thermoplastic matrix, diffraction also increased (see Fig. 3a and b). This can be explained considering that cellulose I is the most common variety found in plants and is characterized by two well-defined peaks at around  $2\theta=22.5^\circ$  and  $2\theta=12.5^\circ$  (Panthapulakkal and Sain 2012).

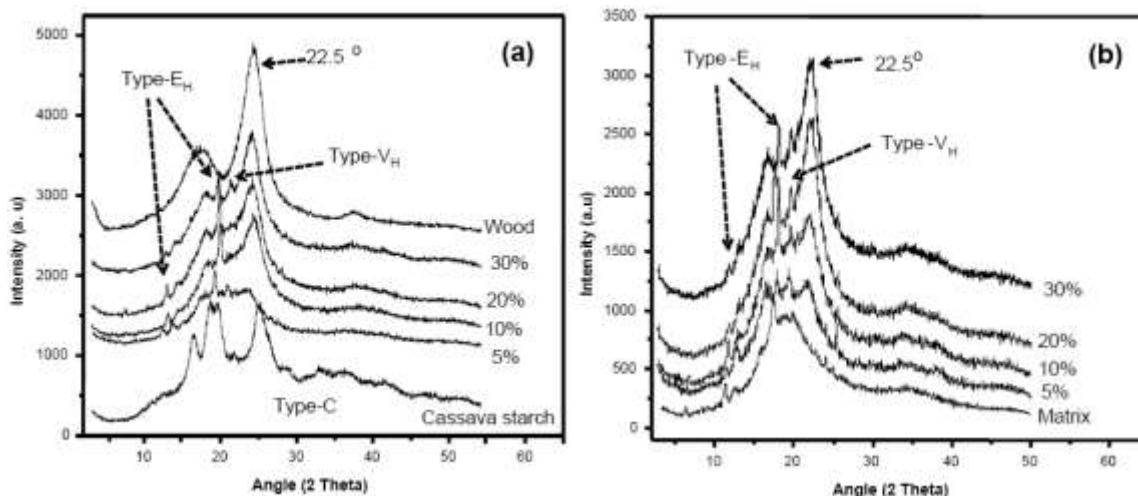


**Fig. 3.** XRD diffractograms of: (a) samples of cassava starch, bio-composites with a particle size of 8 mm, and eucalyptus wood; and (b) samples of matrix and bio-composites with a particle size of 4 mm.



## Moisture Absorption

Sensitivity of the composites to environmental humidity may be one of the most important parameters to consider for some applications, as humidity affects the properties of starch-based composites (Müller *et al.* 2009). Figure 4 shows the plots of moisture absorption as a function of time of both the matrix and bio-composite samples with different particle contents (5 to 30%) exposed to a relative humidity of 75%. Bio-composites with a particle size of 8 mm are depicted in Fig. 4a, while bio-composites with a 4-mm particle size are shown in Fig. 4b. In both cases, a rapid moisture uptake (5 to 7%) can be observed in the first 3 days for all samples, when equilibrium being reached after the 6<sup>th</sup> day (moisture content of 7 to 10%). Matrix samples adsorbed more water than did the bio-composites (see Figs. 4a and 4b). This behavior can be attributed to the polysaccharide composition of the starch (amylose and amylopectin), with a considerable amount of OH groups that easily adhere to water molecules by hydrogen bonding (Corradini *et al.* 2005). In contrast, the moisture absorption decreased when the percentage of wood particles increased in the bio-composites (5 to 30%). According to Sarifuddin *et al.* (2012), this moisture absorption reduction in bio-composites can be attributed to stronger hydrogen bonds between the matrix and the reinforced material. Furthermore, Müller *et al.* (2009) demonstrated the resistance to water absorption in TPS when cellulose fibers are incorporated. In fact, they proposed the incorporation of fibers in TPS as an alternative for reducing water uptake in bio-composites exposed to high-humidity environments. This behavior is also confirmed in Table 2, where the maximum percentage values of moisture absorption (equilibrium) of the matrix and bio-composite samples at 75% humidity are shown.

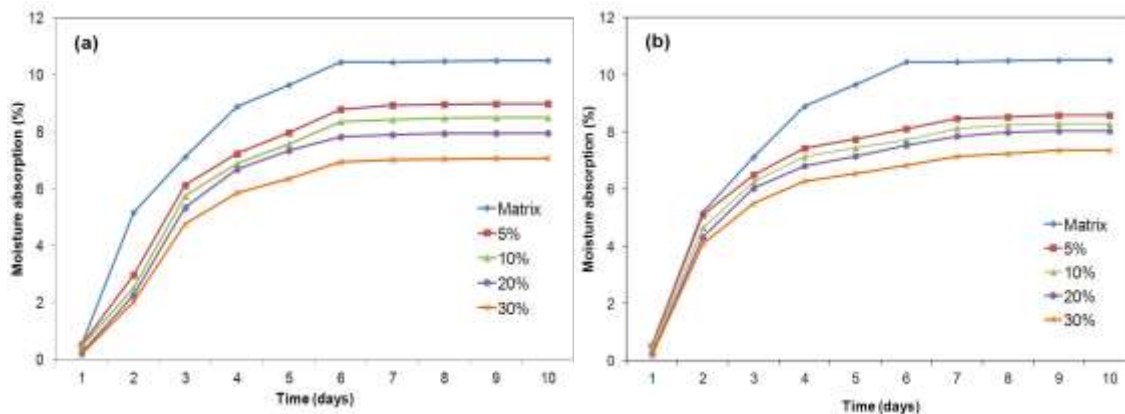


**Fig. 4.** Moisture absorption plots of the matrix and bio-composites with: (a) an 8-mm particle size and (b) a 4-mm particle size

Although moisture absorption reached equilibrium, bio-composites (5 and 10%) with a 4-mm particle size seemed to absorb less water (Fig. 4b) than bio-composites with a particle size of 8 mm and equal amounts of wood particles (Fig. 4a). No significant differences were found in bio-composites with 20 and 30% particle content for both particle sizes (less than 1% of absorbed moisture between them), as can be observed in Table 2. Ma *et al.* (2005) reported values of 37% moisture absorption at equilibrium for thermoplastic matrices of corn starch and 21 to 25% for bio-composites with fiber amounts between 5 and 20% at a relative humidity of 75%. However, similar corn starch thermoplastics with 5 to 30% sisal fibers reached 28 to 32% moisture content at 97% relative humidity (Corradini *et al.* 2008). Those investigations demonstrate that

differences in the moisture absorption at equilibrium for different materials that have been amplified with TPS depends on the starch source, fibers or reinforcing material content, the amount and kind of plasticizer used, and the relative humidity value.

**Table 2.** Moisture Absorption Values at Equilibrium of Matrix and Bio-composites (5 to 30%) with 8-mm and 4-mm Particle Sizes

Material	Moisture percentage in equilibrium	
	Particle size 8 ± 1 mm	Particle size 4 ± 1 mm
Matrix	10.4	
5%	8.9	8.5
10%	8.4	8.2
20%	7.9	7.9
30%	7.0	7.2

### FTIR Spectroscopy

Chemical characterization of the starch, matrix, and bio-composites with different sizes and amounts of particles was evaluated by FTIR. In Table 3, the principal signal assignments are listed (Kizil *et al.* 2002; Pretsch *et al.* 1989; Sarifudin *et al.* 2012) according to the FTIR spectra obtained. Figure 5 shows the spectra of the initial starch and matrix used for preparing the bio-composites. The starch spectrum shows the common signals for these kinds of polysaccharides, with glucopyranose rings such as O-H bands at 3300 cm<sup>-1</sup>, C-H stretching vibrations of aliphatic groups at 2926 cm<sup>-1</sup>, adsorbed water signals at 1650 cm<sup>-1</sup>, C-C and C-O stretching at 1160 cm<sup>-1</sup>, and C-O-H bending vibration at 1005 cm<sup>-1</sup>. In the matrix spectrum, some signals were slightly shifted in comparison with the starch, as can be observed in Table 3. New signals appeared at 1715 and 1264 cm<sup>-1</sup>, the first of which was due to C=O stretching vibration, and the second of which was due to CH<sub>2</sub>-OH side chains. This carbonyl signal (C=O) can possibly be attributed to carboxylic acid, ketone, or aldehyde groups.

**Table 3.** Signal Assignments for FTIR Spectra of Cassava Starch, Matrix, and Bio-composites

Infrared signal assignment	Signal frequencies (cm <sup>-1</sup> )		
	Cassava starch(s) and matrix (m)	Composites with particles of 4 mm	Composites with particles of 8 mm
O-H stretch	3300 <sup>s</sup> and 3270 <sup>m</sup>	3310	3300
C-H stretch	2926	2930	2930
C=O stretch	1715 <sup>m</sup>	1720	1720
H <sub>2</sub> O absorbed	1650 <sup>s</sup> and 1640 <sup>m</sup>	1646	1640
CH <sub>2</sub> -OH side chain	1264 <sup>m</sup>	1240	1245
C-O C-C stretch	1160	1160	1160
C-O-H bend	1005	1010	1015

The side chain signal of alcohol is presumed to have originated from the glycerine added to the matrix or from the CH<sub>2</sub>-OH of the C<sub>6</sub> in the glucopyranose rings of the starch. Because this signal at 1264 cm<sup>-1</sup> is better observed in the matrix spectrum than in

the starch, it can be expected that the principal contribution is from the C-OH of glycerol. On other hand, the carbonyl signal is not expected to appear in either the starch or matrix samples because the chemical composition of neither the original starch nor the mixture of starch and glycerol (matrix) has any carbonyl groups in its chemical structure. Nevertheless, the bio-composites and the matrix were prepared by a thermal laminating process, which can trigger the decomposition of the starch during treatment. This decomposition produces carbonyl compounds such as aldehydes, ketones, and carboxylic acids. However, the low level of decomposition does not affect the physicomechanical properties of the bio-composites, as has been previously reported (Lomelí-Ramírez *et al.* 2014).

The spectra of bio-composites with different eucalyptus particle content amounts (5, 10, 20, and 30%) and organized by particle sizes of 4 mm and 8 mm are depicted in Fig. 6a and b, respectively. In both cases, similar signal patterns are observed (Table 3) from bio-composites prepared with 4-mm (Fig. 6a) and 8-mm particle sizes (Fig. 6b) as a result of their similar chemical composition. However, changes in the intensity of some signals, such as those at 1715, 1640, and 1240 ( $\pm 5$ )  $\text{cm}^{-1}$ , can be attributed to the amount and size of the particles. In the case of the bio-composites prepared with a 4-mm particle size, the signal at 1720  $\text{cm}^{-1}$  decreased when the amount of particles increased. The amount of adsorbed water seemed to have a small increase in the bio-composite that had a 30% particle amount. However, this may be only an optical effect caused by the decrease of the adjacent carbonyl band (1720  $\text{cm}^{-1}$ ). In contrast, the signal at 1240  $\text{cm}^{-1}$  decreased when the amount of particles was 20 and 30%.

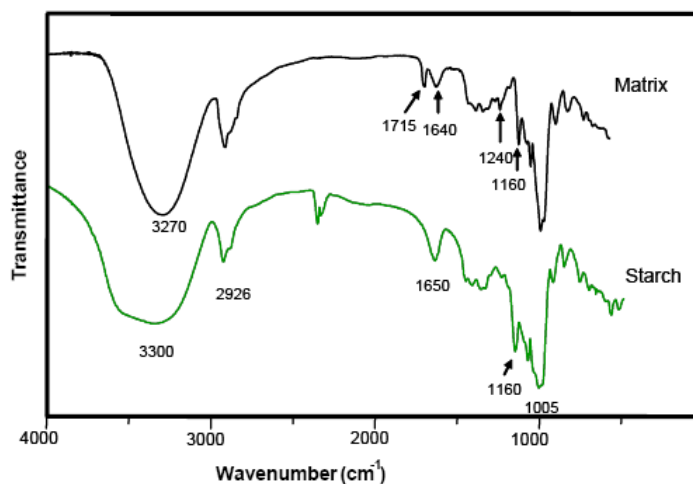


**Fig. 5.** FTIR spectra of native cassava starch and matrix

Although the carbonyl signal (1720  $\text{cm}^{-1}$ ) of bio-composites prepared with particles of 8 mm (Fig. 6b) was more intense than that of the bio-composites prepared with particles of 4 mm (Fig. 6a), both showed similar behavior in terms of decreasing signal intensity when the particle content increased. This is clearly due to a decrease in the amount of matrix in the bio-composites. Moreover, the signal at 1245  $\text{cm}^{-1}$  showed an intense and sharp band of up to 20% particles of 8 mm, and it almost disappeared when the amount of these particles reached 30%. A possible explanation for this may be hydrogen bonding between the  $\text{CH}_2\text{-OH}$  groups from the starch and glycerol with the

wood particles (Sarifudin *et al.* 2012). This association can explain the compatibility between matrix and wood particles observed in the micrographs of the bio-composites in Fig. 1.

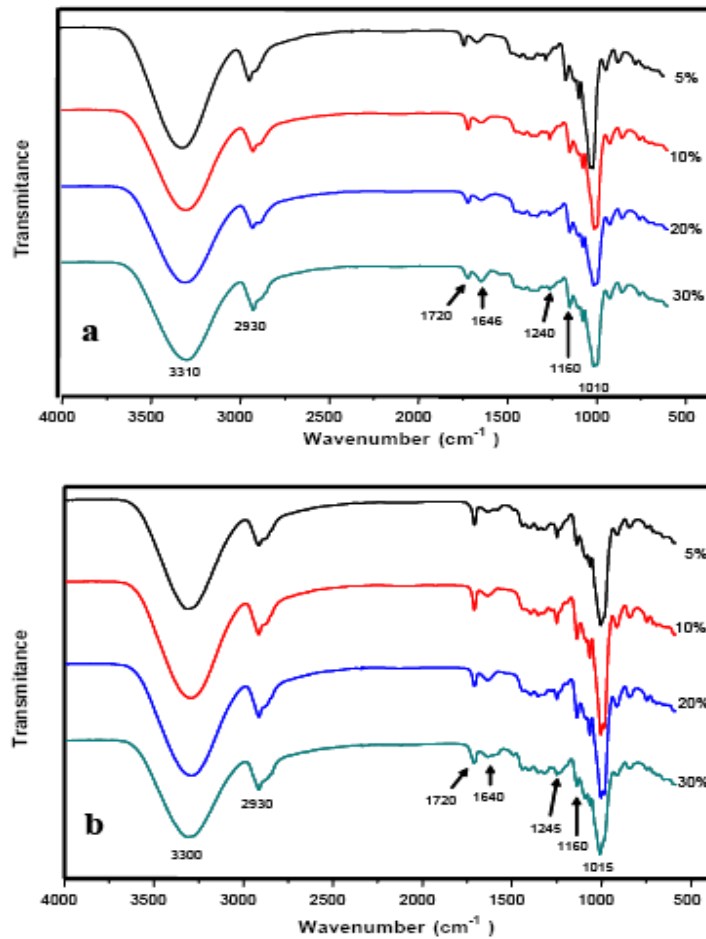


**Fig. 6.** FTIR spectra of bio-composites with different amounts of particles (5 to 30%): (a) particle size of 4 mm and (b) particle size of 8 mm

## CONCLUSIONS

1. In the present study, a preparation process for bio-composites of thermoplastic cassava starch and eucalyptus particles with sizes of 4 and 8-mm, at different particle amounts (5 to 30%), demonstrated viability by direct thermal compression, avoiding the common problems of high viscosity present in traditional injection or extrusion processes.
2. The tensile strength and elasticity modulus of the bio-composites increased with the addition of eucalyptus particles (5 to 30%). Bio-composites prepared with a smaller particle size (4 mm) showed the best tensile properties because of a better adhesion between the matrix and particles.

3. Moisture absorption values decreased in inverse proportion to the amount of wood particles incorporated in the matrix. The effect of the size of the particles in bio-composites with similar particle contents was not significant (< 1%).
4. A direct plasticization process using temperature, pressure, and a plasticizer triggered granular disruption, which changed the characteristics of the starch profile from type C<sub>A</sub> to type E<sub>H</sub> and type V<sub>H</sub>. Parameters such as temperature and time applied during the bio-composite preparation contributed to the formation of the predominant crystallographic diffraction patterns V<sub>H</sub> and E<sub>H</sub>.
5. FTIR analyses demonstrated chemical compatibility between glycerol and cassava starch in matrix samples, as well as with eucalyptus particles in all bio-composites, which were attributed to the association by hydrogen bonding of OH moieties of starch, glycerol, and the cellulose of the wood particles. Bio-composites prepared with different amounts of eucalyptus particles and two different particle sizes showed similar patterns. Small amounts of carbonyl groups caused by the thermal degradation of thermal compression were formed in the matrix and bio-composite samples. However, this decomposition did not affect the mechanical properties of the composites.
6. Finally, the results of this study contribute important information concerning the development of new biodegradable composites with practical application for diverse purposes such as alternatives for the plastics industry, packing containers, eating utensils, and furniture production.

## REFERENCES CITED

- Alemdar, A., and Sain, M. (2008). "Biocomposites from wheat straw nanofibers; Morphology, thermal, and mechanical properties," *Composites Science and Technology* 68(2), 557-565.
- ASTM E104-02. (2007). "Standard practice for maintaining constant relative humidity by means of aqueous solutions," Book of Standards Volume 11.07, USA. 5p.
- ASTM D638M-96. (1998). "Standard test method for tensile properties of plastics," Book of Standards Volume 08.01, USA. 16p.
- Avérous, L., and Halley, P. J. (2009). "Biocomposites based on plasticized starch," *Biofuels, Bioproducts and Biorefining* 3(3), 329-343.
- Bilbao-Sainz, C., Bras, J., Williams, T., Sénechal, T., and Orts, W. (2011). "HPMC reinforced with different cellulose nano-particles," *Carbohydrate Polymers* 86(4), 1549-1557.
- Canevarolo, S. V. (2006). "Ciência dos polímeros," Estrutura molecular do estado sólido. Artliber Editora Ltda, São Paulo, Brazil. 91-127.
- Chakraborty, A., Sain, M., Kortschot, M., and Cutler, S. (2007). "Dispersion of wood microfibrils in a matrix of thermoplastic starch and starch-poly(lactic acid) blend," *Journal of Biobased Materials and Bioenergy* 1(1), 71-77.
- Corradini, E., Lotti, C., Medeiros, E. S., Carvalho, A. J. F., Curvelo, A. A. S., and Mattoso, L. H. C. (2005). "Estudo comparativo de amidos termoplásticos derivados do milho com diferentes teores de amilose," *Polímeros: Ciência e Tecnologia* 15(4), 268-273.

- Corradini, E., de Morais, L. C., Rosa, M., Mazzetto, S. E., Mattoso, L. H. C., and Agnelli, J. A. M. (2006). "A preliminary study for the use of natural fibers as reinforcement in starch-gluten-glycerol matrix," *Macromolecular Symposia* 245-246(1), 558-564.
- Corradini, E., Agnelli, J. A. M., de Morais, L. C., and Mattoso, L. H. C. (2008). "Estudo das propriedades de compósitos biodegradáveis de amido/glúten de milho/glicerol reforçados com fibras de sisal," *Polímeros: Ciência e Tecnologia* 18(4), 353-358.
- Duanmu, J., Gamstedt, E. K., Pronovich, A., and Rosling, A. (2010). "Studies on mechanical properties of wood fiber reinforced cross-linked starch composites made from enzymatically degraded allyl glycidyl ether-modified starch," *Composites Part A: Applied Science and Manufacturing* 41(10), 1409-1418.
- Espinach, F. X., Julián, F., Alcalá, M., Tresserras, J., and Mutjé, P. (2014). "High stiffness performance alpha-grass pulp fiber reinforced thermoplastic starch-based fully biodegradable composites," *BioResources* 9(1), 738-755.
- Fowler, P. A., Hughes, J. M., and Elias, R. M. (2006). "Biocomposites: Technology, environmental credentials and market forces," *Journal of the Science of Food and Agriculture* 86(12), 1781-1789.
- Guimarães, J. L., Wypych, F., Saul, C. K., Ramos, L. P., and Satyanarayana, K. G. (2010). "Studies of the processing and characterization of corn starch and its composites with banana and sugarcane fibers from Brazil," *Carbohydrate Polymers* 80(1), 130-138.
- Kawabata, A., Sawayama, S., Nagashima, N., Rosario, R. R., and Nakamura, M. (1984). "Some physicochemical properties of tropical starches," *Journal of the Japanese Society of Starch Science* 31(4), 224-232.
- Kizil, R., Irudayaraj, J., and Seetharaman, K. (2002). "Characterization of irradiated starches by using FT-Raman and FTIR spectroscopy," *Journal of Agricultural and Food Chemistry* 50(40), 3912-3918.
- Kuciel, S., and Liber-Knec, A. (2009). "Biocomposites on the base of thermoplastic starch filled by wood and kenaf fiber," *Journal of Biobased Materials and Bioenergy* 3(3), 269-274.
- Liu, D., Zhong, T., Chang, P. R., Li, K., and Wu, Q. (2010). "Starch composites reinforced by bamboo cellulosic crystals," *Bioresource Technology* 101, 2529-2536.
- Lomelí Ramirez, M. G., Satyanarayana, K. G., Iwakiri, S., de Muniz, G. B., Tanobe, V., and Flores-Sahagun, T. S. (2011). "Study of the properties of biocomposites: Part I - Cassava starch-green coir fibers of Brazil," *Carbohydrate Polymers* 86(4), 1712-1722.
- Lomelí Ramirez, M. G., Satyanarayana, K. G., Manríquez, G. R., Iwakiri, S., de Muniz, G. B., and Flores-Sahagun, T. S. (2014). "Bio-composites of cassava starch-green coconut fiber: Part II-Structure and properties," *Carbohydrate Polymers* 102(15), 576-583.
- Ma, X., Yu, J., and Kennedy, J. F. (2005). "Studies on the properties of natural fibers reinforced thermoplastic starch composites," *Carbohydrate Polymers* 62(1), 19-24.
- Müller, C. M. O., Laurindo, J. B., and Yamshita, F. (2009). "Effect of cellulose fibers on the crystallinity and mechanical properties of starch-based films at different relative humidity values," *Carbohydrate Polymers* 77(2), 293-299.
- Panthapulakkal, S., and Sain, M. (2012). "Preparation and characterization of cellulose nanofibril films from wood fibre and their thermoplastic polycarbonate composites," *International Journal of Polymer Science* 2012, 1-6.

- Prachayawarakorn, J., Sangnitdej, P., and Boonpasith, P. (2010). "Properties of thermoplastic rice starch composites reinforced by cotton fiber or low-density polyethylene," *Carbohydrate Polymers* 81(2), 425-433.
- Pretsch, E., Clerc, T., Seibil, J., and Simon, W. (1989). *Tables of Spectral Data for Structure Determination of Organic Compounds: 13C-NMR, 1H-NMR, IR, MS, UV/VIS Chemical Laboratory Practice*. Fresenius, W., Huber, J. F. K., Pungor, E., Rechnitz, G. A., Simon, W., and West, T. S. (eds.), 2<sup>nd</sup> edition, Springer-Verlag, Berlin, 15-280.
- Sarifuddin, N., Ismail, H., and Ahmad, Z. (2012). "Effect of fiber loading on properties of thermoplastic sago starch/kenaf core fiber biocomposites," *BioResources* 7(3), 4294-4306.
- Teixeira, E. M., Pasquin, D., Curvelo, A. A. S., Corradini, E., Belgacem, M. N., and Dufresne, A. (2009). "Cassava bagasse cellulose nanofibrils reinforced thermoplastic cassava starch," *Carbohydrate Polymers* 78(3), 422-431.
- van Soest, J. J. G., Hulleman, S. H. D., de Wit, D., and Vliegthart, J. F. G. (1996). "Crystallinity in starch bioplastics," *Industrial Crops and Products* 5(1), 11-22.
- Vilaseca, F., Méndez, J. A., Pelach, A., Llop, M., Cañigüeral, N., Girones, J., Turon, X., and Mutjé, P. (2007). "Composite materials derived from biodegradable starch polymer and jute strands," *Process Biochemistry* 42(3), 329-334.
- Wicaksono, R., Syamsu, K., Yuliasih, I., and Nasir, M. (2013). "Cellulose nanofibers from cassava bagasse: Characterization and application on tapioca-film," *Chemistry and Materials Research* 3(13), 79-87.
- Zobel, H. F. (1988). "Starch crystal transformations and their industrial importance," *Starch/Stärke* 40(1), 1-7.

Article submitted: January 31, 2014; Peer review completed: March 30, 2014; Revised version received: April 1, 2014; Accepted: April 3, 2014; Published: April 8, 2014.